IEEE Photonics Journal
An IEEE Photonics Society Publication

Open Access

Effect of CO_2 Laser Annealing on Stress Applying Parts Contributing Toward Birefringence Modification in Regenerated Grating in Polarization Maintaining Fiber

Volume 7, Number 5, October 2015

Man-Hong Lai
Kok-Sing Lim
Md. Rajibul Islam
Dinusha S. Gunawardena
Hang-Zhou Yang
Harith Ahmad

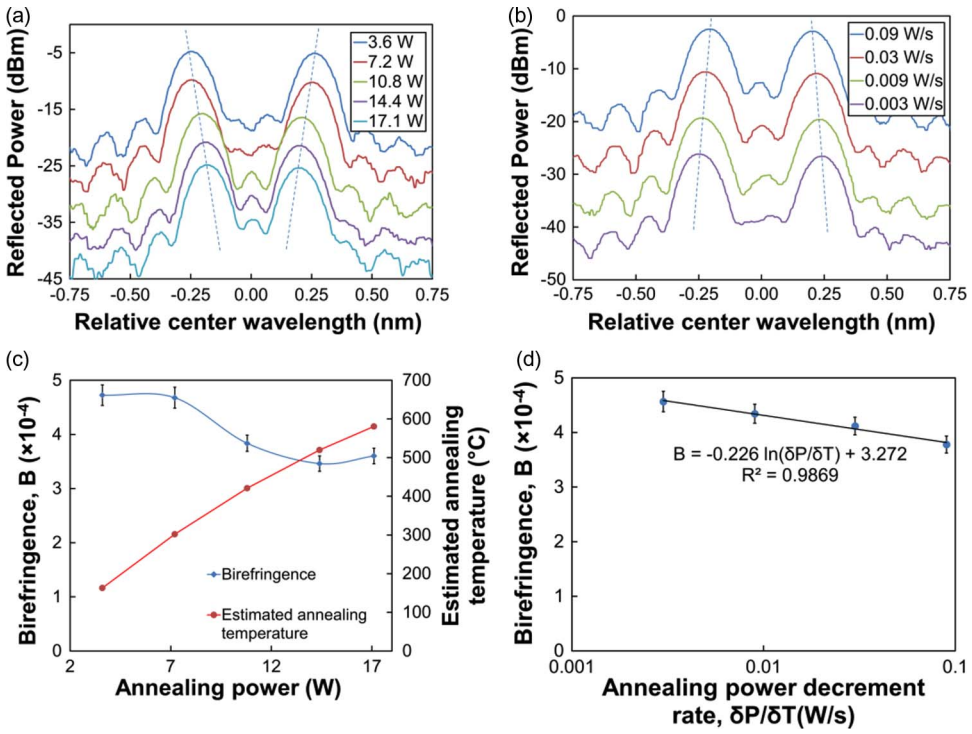

DOI: 10.1109/JPHOT.2015.2477496
1943-0655

IEEE photonics SOCIETY

IEEE

Effect of CO_2 Laser Annealing on Stress Applying Parts Contributing Toward Birefringence Modification in Regenerated Grating in Polarization Maintaining Fiber

Man-Hong Lai,[1] Kok-Sing Lim,[1] Md. Rajibul Islam,[1] Dinusha S. Gunawardena,[1] Hang-Zhou Yang,[2] and Harith Ahmad[1]

[1]Photonics Research Centre, University of Malaya, 50603 Kuala Lumpur, Malaysia
[2]School of Physics, Northwest University, Xi'an 710069, China

DOI: 10.1109/JPHOT.2015.2477496

Manuscript received July 21, 2015; revised September 4, 2015; accepted September 7, 2015. Date of publication September 9, 2015; date of current version September 23, 2015. This work was supported in part by the University of Malaya through UMRG under Grant RG326-15AFR, through HIR under Grant UM.C/625/1/HIR/MOHE/SCI/01, and through PRGS under Grant PR001-2015A; and in part by the National Natural Science Foundation of China under Grant 61405160. Corresponding author: K. S. Lim (e-mail: kslim@um.edu.my).

Abstract: In this paper, we have demonstrated birefringence modification in regenerated grating in polarization maintaining fiber (RGPMF) by using a CO_2 laser annealing technique. After conducting an isothermal annealing procedure followed by a slow cooling process, the birefringence of the RGPMF has been increased. This phenomenon can be explained by the changes in the thermal expansion coefficient and glass transition temperature of the stress applying part at different cooling rates. This process was reversible by reannealing with a subsequent fast cooling process. In our observation, the birefringence exponentially increases with a decreasing cooling rate. The highest and lowest records in the birefringence throughout the annealing process are 4.72×10^{-4} and 3.46×10^{-4}, respectively (a difference of 1.26×10^{-4}). This finding is useful for the study of the birefringence modification, measurement range, sensitivity, and accuracy of PMF or PMF-related devices.

Index Terms: Fiber optics and optical communications, fiber Bragg gratings, all-optical devices.

1. Introduction

High birefringence fiber, which is also known as polarization maintaining fiber (PMF), is widely used as polarizers, depolarizers, couplers, filters, isolators, polarization controllers, and sensors. Birefringence in PMF can be categorized into geometrical birefringence and stress-induced birefringence. Generally, the geometrical birefringence is much smaller than the stress-induced birefringence, also known as material birefringence, exerted by the dopant concentration difference between each region in the fiber cross section [1]. Generally, stress applying parts (SAP) that position at both sides of the fiber core provide better precision in

controlling the birefringence and fabrication of PMF. The birefringence of stress-applied PMF can be described using

$$B \cong K(\alpha_{\text{clad}} - \alpha_{\text{SAP}})\Delta T \tag{1}$$

$$\Delta T = T_{\text{room}} - T_{\text{g(SAP)}} \tag{2}$$

where α_{clad} and α_{SAP} represent the thermal expansion coefficients (TEC) of the cladding and stress applying part (SAP), respectively; T_{room} and $T_{\text{g(SAP)}}$ represent the room temperature and glass transition temperature of SAP; and K is the fiber geometry constant which is defined by the fiber radius, dimension, and position of SAPs in the fiber [1].

During the drawing process of PMF, high mechanical stresses are induced in the fiber due to the high drawing tensions, and the stresses are permanently frozen in the fiber at room temperature. As the result, a compensating thermal stress is formed in the fiber core region, which leads to a lower stress induced birefringence [2]. Nonetheless, the thermal annealing treatment can serve as a remedy to reducing frozen mechanical stresses and enhancing the birefringence in the fiber. The remaining stresses in fiber are purely thermal stress, which is usually observed in the tension free fiber preform [3]. Besides the thermal relaxation of mechanical stress, the enhancement of birefringence can also be achieved by modifying the TEC of SAPs by means of thermal annealing treatment followed by a slow cooling process [4], [5]. The slow cooling process provides sufficient relaxation time for the molecular rearrangement at low-viscous state and eventually leads to the volume compaction of SAP. The T_g and TEC of the glass are affected by the cooling process after annealing at elevated temperature. Silica glass that is cooled at a slower rate has a lower T_g and a smaller volume [6], [7] but a higher TEC compared to that of rapidly cooled [8]. This can be attributed to the rearrangement of molecular structure of the glass matrix and the free volume model of amorphous material [9]. Slow cooling from the annealing temperature introduces lesser free volume in the molecular structure. In other words, higher compaction in volume is achieved at a slower cooling rate [10]. Therefore, higher stress-applied birefringence can be achieved. However, this process is reversible by repeating the annealing treatment, and then, birefringence is induced in the fiber core due to the smaller product of ΔT and TEC mismatch between SAPs and cladding after fast cooling.

FBGs inscribed on birefringent optical fibers have been reported in several studies using elliptical core [11], bow-tie [12], Panda [13], and internal elliptical cladding [14]. The spacing between the two Bragg wavelengths $(\Delta\lambda_B)$ in birefringent optical fiber can be described by $\Delta\lambda_B = \delta n \cdot \wedge_{\text{pm}}$ where $\Delta\lambda_B$ is the wavelength difference between the polarization modes and $\wedge_{\text{pm}}$ is the phase mask period [15]. Chehura *et. al.* [16] demonstrated FBGs inscribed on elliptically clad fiber with a high transverse load sensitivity of 0.23 $\pm$ 0.02 nm/(N/mm) ($\sim$25% higher than any other PMF). This makes it an ideal embedded or surface mounted strain sensor. On the other hand, highest temperature sensitivity of 16.5 $\pm$ 0.1 pm$^{\circ}$C^{1} ($\sim$27% greater than any other fiber type) was reported for a FBG sensor inscribed on Panda type PMF [16]. In addition, simultaneous monitoring of strain and temperature was demonstrated using PMF with referral to the different dependences of two orthogonal polarization modes [17], [18]. Multi-axis strain sensing based on PMF is possible and has been demonstrated in [19]–[21]. The measurement of three independent components of strain and temperature can be achieved by using two gratings with center wavelengths sufficiently spaced in the spectrum but co-locate at the same position on a PMF [21]. Taking advantage of the two orthogonal modes in PMF, grating in PMF can be used for the generation of dual-wavelength laser and single linearly polarized laser [22]–[25].

The stochastic behavior of birefringence in PMF due to different thermal history has been reported in [4]. The birefringence change due to this stochastic behavior is indistinguishable from the spectral change caused by the sensing parameter [26]. Furthermore, lower birefringence limits the measurable range of the high birefringent fiber sensor. For example, the two reflection peaks that correspond to the two orthogonal modes overlap with each other when the applied strain induces more wavelength shift than the Bragg wavelength spacing [19]. Beside high-birefringent grating

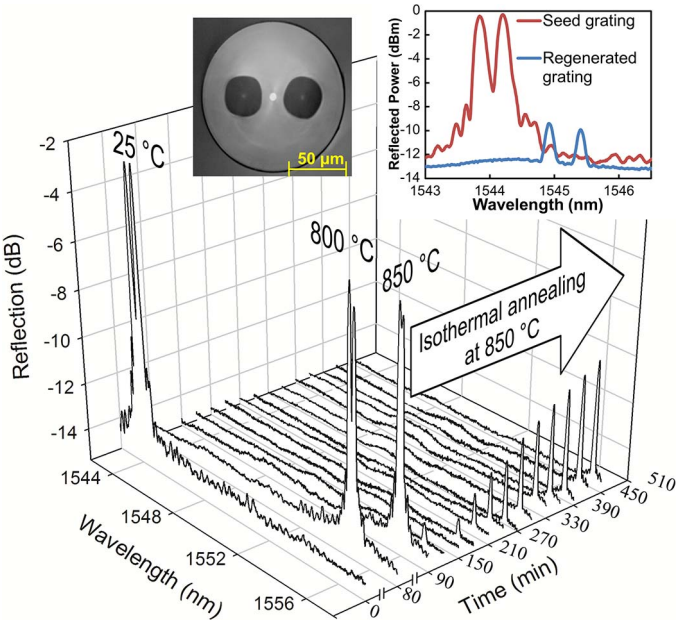

Fig. 1. Spectral evolution of PMF during regeneration process. (Inset) Reflection spectrum of seed grating and regenerated grating written in PMF. The micrograph shows the cross section of PMF (SAP diameter ~33 μm).

sensors, the performance of interferometric sensors based on PMF also strongly relies on the fiber birefringence [5], [27], [28]. Therefore, post-manufacture modification of birefringence in PMF by means of thermal-annealing treatment provides an appealing approach for controlling and improving the performance of high birefringent fiber sensor in terms of detection range and sensitivity.

In comparison with the thermal annealing technique using a conventional furnace, CO_2 laser annealing offers the advantages of dynamic control, flexibility in the manipulating annealing area, and rapid thermal response. The mechanical stress relaxation by CO_2 laser annealing is widely employed in long period grating (LPG) fabrication. Thermal stress modification in Ge/B co-doped photosensitive fiber with the usage of CO_2 laser has been reported in our previous work [10]. Hence, CO_2 laser annealing is a good candidate for the birefringence modification in high birefringent fiber.

In this work, birefringence modification by CO_2 laser annealing in panda type PMF is demonstrated and studied. The grating in PMF was first inscribed with the employment of KrF excimer laser and subsequently regenerated using high temperature furnace. The produced high temperature resistant grating was later annealed using CO_2 laser with different annealing powers and cooling rates. The high temperature resistant characteristic of regenerated grating in Polarization Maintaining Fiber (RGPMF) makes it a good candidate for the investigation of birefringence modification by thermal annealing without degradation in grating strength. The birefringence changes were observed, calculated, and analyzed based on the spectral change of the grating after each thermal treatment in order to investigate the relationship between the thermal history and birefringence of PMF.

2. Experiment

2.1. Regenerated Grating in Polarization Maintaining Fiber (RGPMF) Fabrication

In the preparation, photosensitive panda type polarization maintaining fiber (Thorlabs PS-PM980) was hydrogenated under the pressure of 1500 psi at room temperature for a week. The cross sectional micrograph of this fiber is shown in the inset of Fig. 1. Subsequently, a 5-mm-long uniform

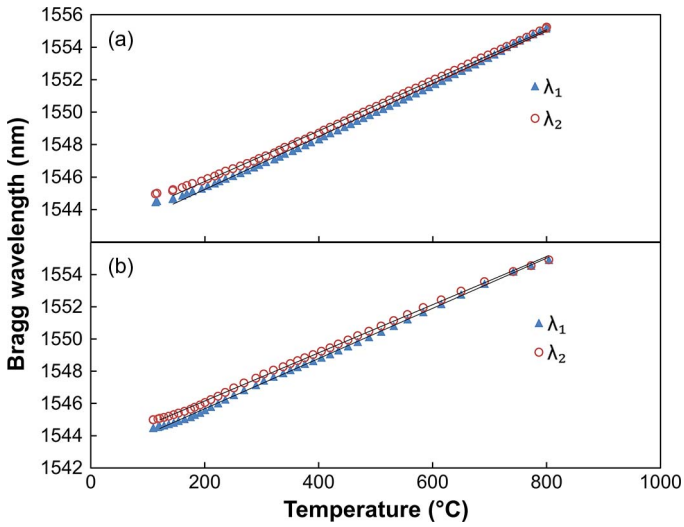

Fig. 2. Thermal calibration of RGPMF (a) heating-thermal sensitivity of 15.6 pm/°C for λ_2 and 16.3 pm/°C for λ_1 and (b) cooling-thermal sensitivity of 14.9 pm/°C for λ_2 and 15.6pm/°C for λ_1. λ_1 (▲): Fast axis Bragg wavelength. λ_2 (○): Slow axis Bragg wavelength.

grating was inscribed in the PMF using KrF excimer laser (248 nm) based on fixed beam/phase mask lithography technique, followed by the dehydrogenation procedure using oven (80 °C for ∼8 hours). The fiber was fixed on the stage using fiber holders throughout the grating inscription process. Afterwards, thermal regeneration of the seed grating was performed by using a high temperature tube furnace (LT Furnace STF25/150–1600). During the regeneration process, the annealing temperature was increased in steps from room temperature to ∼850 °C, with a step size of ∼10 °C every minute. The grating strength decayed slowly until it was completely diminished. Shortly after that, a progressive growth was observed and stabilization was achieved after 7–8 hours. It was observed that the birefringence of PMF was reduced to zero at ∼850 °C (see Fig. 1). This indicates the complete elimination of SAP-induced stress in the fiber core due to viscosity reduction in the SAP at high temperature. Due to high concentration of Boron dopant in SAP (∼7.32 wt%), the glass transition temperature of SAP is lower and stress relaxation occurs at lower temperature than that in fiber core. After the onset of regeneration process at ∼850 °C, the reflection peak decayed to below the noise level. It took ∼30 minutes for the formation of a new grating and an additional 7–8 hours for the regrowth and stabilization of the regenerated grating. Thereupon, the furnace was switched off and the produced RFBG was left in the furnace to cool down to room temperature. The birefringence was re-introduced into PMF during the cooling process after grating regeneration because of the increment in viscosity of SAP. Fig. 1 shows that, the birefringence increases from 3.37×10^{-4} to 4.56×10^{-4} after regeneration process based on the Bragg wavelength spacing between two orthogonal modes. This is due to the longer cooling process (slower cooling rate) after the regeneration treatment, as compared to the quenching rate during fiber pulling. Therefore, the compaction (or volume shrinkage) in SAPs due to slower cooling rate enhances the birefringence. Besides that, a red shift in Bragg wavelength was observed after regeneration instead of the blue shift which was observed in the non polarization maintaining fiber. The slow cooling process after the regeneration might be the reason for the red shift in Bragg wavelength, which is due to the thermal stress relaxation [10].

Thermal calibration of RGPMF was carried out using high temperature furnace from room temperature to 800 °C. The plots of Bragg wavelengths for both orthogonal polarization modes against temperature are presented in Fig. 2. During heating process, the thermal sensitivity of Bragg wavelengths in fast and slow axes are 15.6 pm/°C and 16.3 pm/°C, respectively, whereas, during the cooling process, the thermal sensitivity of Bragg wavelengths in fast and

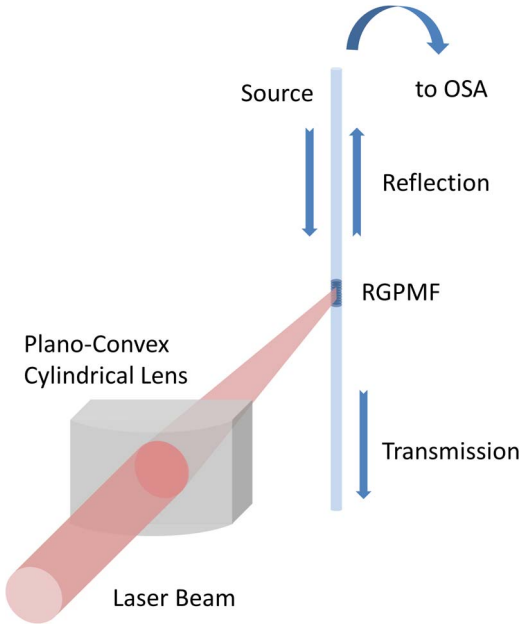

Fig. 3. Schematic diagram of CO_2 laser annealing setup.

slow axes are 14.9 pm/°C and 15.6 pm/°C, respectively. Generally, the slow axis Bragg wavelength has a higher thermal sensitivity compared to the fast axis Bragg wavelength. For this reason, the two Bragg wavelengths merge at high temperature (∼850 °C), where the birefringence eventually reduces to zero. In the comparison with the grating before regeneration, the temperature sensitivities for both axes are ∼16.2 pm/°C. This shows that the temperature sensitivity of the grating does not change after the regeneration process. The maximum operating temperature of the regenerated grating in polarization maintaining fiber is close to its regeneration temperature (∼850 °C). At regeneration temperature, the birefringence of the grating completely disappears making the grating to lose its ability in multiparameter sensing. At this stage, the grating will behave like a grating in single mode fiber. Further increase in temperature to beyond 1000 °C will result in a permanent decay of the grating strength of the grating and inaccurate temperature measurements.

2.2. CO_2 Laser Annealing

The CO_2 laser annealing technique demonstrated in our previous work [10], [29] is used in this study. Fig. 3 shows the graphical illustration of the experimental setup. The CO_2 laser used for the annealing process is fan-cooled SYNRAD 48-2 SAM. The maximum power of the collimated beam was ∼18 W. The details of laser power increment and decrement rates, isothermal annealing laser power and time used in the investigation are tabulated in Table 1. The estimated temperature in Table 1 was estimated using a thermocouple. During irradiation of the sapphire mini furnace (as mentioned in [29]) with different intensity of CO_2 laser beam, the sensing probe of the thermocouple was placed directly in contact with the sapphire mini furnace in order to measure its current temperature. The estimated annealing temperature shown in Table 1 is the calibrated data from the thermocouple. Two annealing treatments were carried out using RGPMF. In the first annealing experiment, a treatment cycle of F1-F2-F3-F4-F5 was performed. This treatment sequence was applied to investigate the annealing power dependence of birefringence variation in RGPMF. In the second annealing treatment, a sequence of F5-S1-F5-S2-F5-S3-F5-S4 was carried out and the cooling rate dependency of birefringence in RGPMF was investigated.

TABLE 1

Summary of CO_2 laser annealing treatments

Treatment	Laser power increment rate (%/s)	Relative annealing power (%) / estimated temperature (°C)	Annealing time (min)	Laser power decrement rate
F1	1	20 / ~163	5	20% /s
F2	1	40 / ~302	5	20% /s
F3	1	60 / ~421	5	20% /s
F4	1	80 / ~520	5	20% /s
F5	1	95 / ~581	5	20% /s
S1	1	95 / ~581	5	0.5% /s
S2	1	95 / ~581	5	0.5% /3 s
S3	1	95 / ~581	5	0.5% /10 s
S4	1	95 / ~581	5	0.5% /30 s

P/s.: F: Fast cooling, S: Slow Cooling.
Relative annealing power based on the maximum laser output power (18W).

3. Results and Discussion

The slow cooling process results in a smaller volume of SAPs at room temperature, thus increasing the stress induced birefringence in the fiber core [4]. When RGPMF was annealed with a high power CO_2 laser, the stress relaxation occurred in SAP before fiber core. Referring to (1), different cooling rates caused the variations in $T_{g(SAP)}$ and TEC of SAP, which in turn changed the birefringence of RGPMF. A slower cooling rate introduced higher birefringence in RGPMF, which indicated that the product of the difference of ΔT and TEC between cladding and SAP had increased as well. However, the slower cooling process lowers the $T_{g(SAP)}$ [4]. Apparently, the influence of TEC change in SAP to the birefringence by different cooling rates is greater than that of $T_{g(SAP)}$.

Fig. 4 shows the reflection spectrum and birefringence change with different annealing laser power and cooling rate. Fig. 4(a) and (c) show that the birefringence of RGPMF decreases with increasing annealing laser power when a fast cooling rate ($\sim$3.6 W per second) was used. The relationship between the annealing laser power and birefringence change shows a power threshold between 7.2–10.8 W of annealing laser power (estimated temperature 302–421 °C). The highest and lowest birefringences recorded throughout the annealing process are 4.72×10^{-4} and 3.46×10^{-4}, respectively (birefringence difference 1.26×10^{-4}). It marks the onset of the glass transition region, viscosity change, and stress relaxation of the SAPs, where the SAPs are transformed from the glassy state to the rubbery state as the temperature increases. Beyond the glass transition temperature, the viscosity of SAP decreases exponentially with increasing temperature, in accordance to Arrhenius Law. This explains the nonlinear curve in the change of birefringence with annealing power (temperature). On the other hand, Fig. 4(b) and (d) show that the birefringence increases exponentially with decreasing cooling rate. In between each slow cooling treatment (S1, S2, S3, S4), a fast cooling treatment (F5) was performed to reset the birefringence in the RGPMF to the original state. Slower cooling rate enables more compaction in SAPs due to the longer relaxation time.

The birefringence in RGPMF was due to the TEC difference between fiber core and SAPs. The SAP has higher TEC due to its higher dopant concentration. Therefore, a compressive stress was exerted to the fiber core, which causes stress anisotropy in the fiber. The variation in

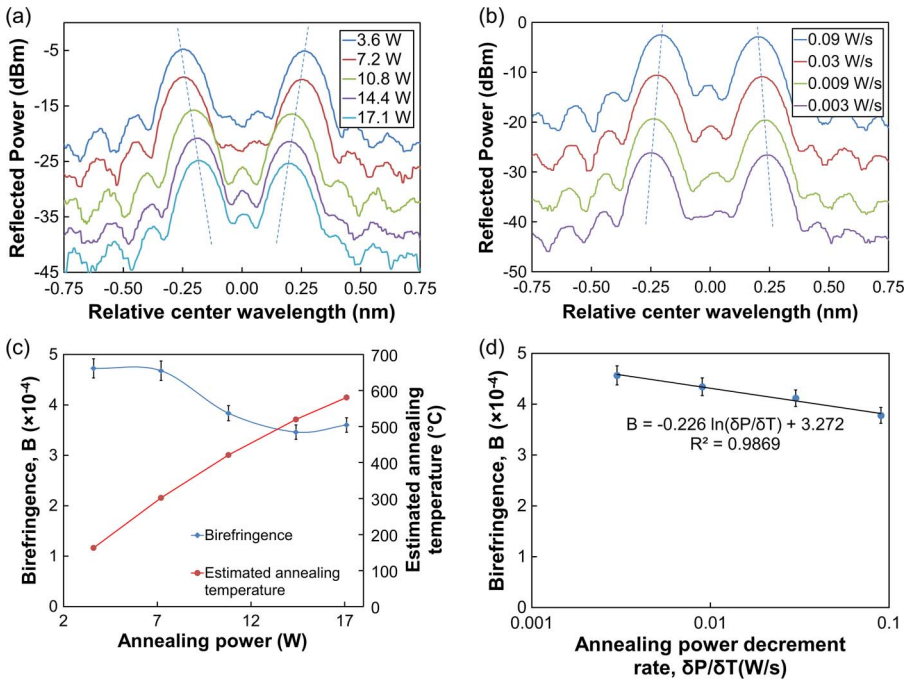

Fig. 4. Spectral response and birefringence variation of RGPMF after the annealing treatments of (a), (c) F1-F5 and (b), (d) S1-S4. The dashed lines in (a) and (b) illustrate the variations of Bragg wavelengths by different treatments.

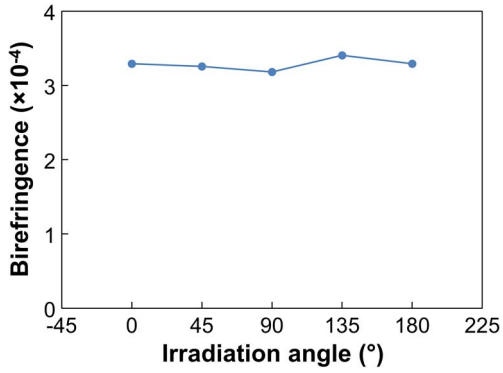

Fig. 5. The birefringence of RGPMF after annealing at different radial direction followed by fast cooling (F5).

birefringence after different cooling processes indicated that the TEC of SAP had been modified. The maximum temperature used for annealing was above the glass transition temperature of SAPs but below that of fiber core. As a result, the stress relaxation is limited to the SAPs. The TEC and glass transition temperature of fiber core in Eqn. (1) are assumed to be constant. The product of TEC and ΔT of SAP was increased with increasing birefringence because of slower cooling rate. Slower cooling promotes stress relaxation in glass structure of SAP, which in turn causes structural compaction due to longer relaxation time. The error of birefringence change due to different annealing process is $\sim$4%. This error might be due to the uncertainty in laser power stability, ambient air turbulence, and alignment of the experimental setup. Additionally, the influence of laser irradiation angle was investigated. The resultant birefringence at different irradiation angles using thermal treatment F5 is shown in Fig. 5. The variation of

birefringence due to different irradiation angles is 2.47%, which is smaller than the observed change in birefringence of 26.8% presented in Fig 4(c). The RGPMF was fixed on the experimental setup throughout the experiment. Hence, the fact of laser direction induced birefringence change can be eliminated from the results obtained.

The CO_2 laser annealing technique provides an easy solution for modification of birefringence in PMF by means of manipulation of annealing rate, cooling rate, and annealing temperature. As a result, this birefringence modification technique makes the birefringence tuning feasible in PMF. This technique can be applied in the fabrication process of PMF as post processing treatment in order to tailor the birefringence of the fiber. Since the high annealing temperature is required, birefringence modification of the fiber Bragg grating is only possible to perform in RGPMF due to its high thermal sustainability. RGPMF is very useful for the application of polarization maintaining in fiber laser operating in a high-temperature environment. RGPMF provides an alternative solution for multi parameter sensing at high temperature. However, in an extremely high-temperature and dynamic environment, the stress relaxation may affect the accuracy in the sensing application.

4. Conclusion

In conclusion, the birefringence modification in RGPMF has been demonstrated using the CO_2 laser annealing technique. The birefringence change is observed after the annealing process where the annealing temperature used is above the interval 302–421 °C. This indicates the onset of glass transition, viscosity change, and the stress relaxation of SAPs where the SAPs are transformed from the glassy state to the rubbery state with increasing temperature. Throughout the entire annealing process, the highest and lowest recorded birefringences are 4.72×10^{-4} and 3.46×10^{-4} respectively (a difference of 1.26×10^{-4}). Besides, it is found that the birefringence increases exponentially with decreasing cooling rate after the annealing process. The variation in $T_{g(SAP)}$ and TEC of the SAPs were responsible for the change in birefringence after each thermal treatment. This work introduces a new technique for modification of birefringence in stress-applied PMF by laser annealing with manipulation of cooling rate. In addition, it offers an appealing approach for improving the thermal sensitivity, dynamic range, and accuracy of RGPMF and other PMF based sensors. Furthermore, the findings in this work provide detailed information for the successful operation of PMF-related devices in a high-temperature and dynamic environment.

References

[1] P. L. Chu and R. A. Sammut, "Analytical method for calculation of stresses and material birefringence in polarization maintaining optical fiber," *J. Lightw. Technol.*, vol. 2, no. 5, pp. 650–662, Oct. 1984.
[2] M. Taccaa, M. Ferrario, P. Boffi, and M. Martinelli, "Drawing parameters optimization for birefringence reduction in optical fibers," *Opt. Commun.*, vol. 283, no. 9, pp. 1773–1776, May 2010.
[3] F. Just *et al.,* "The influence of the fiber drawing process on intrinsic stress and the resulting birefringence optimization of PM fibers," *Opt. Mater.*, vol. 42, pp. 345–350, Apr. 2015.
[4] A. Ourmazd, M. P. Varnham, R. D. Birch, and D. N. Payne, "Thermal properties of highly birefringent optical fibers & preforms," *Appl. Opt.*, vol. 22, no. 15, pp. 2374–2379, Aug. 1983.
[5] A. Ourmazd, R. D. Birch, M. P. Varnham, D. N. Payne, and E. J. Tarbox, "Enhancement of birefringence in polarization maintaining fiber by thermal annealing," *Electron. Lett.*, vol. 19, no. 4, pp. 143–144, Feb. 1983.
[6] C. T. Moynihan, A. J. Easteal, J. Wilder, and J. Tucker, "Dependence of the glass transition temperature on heating and cooling rate," *J. Phys. Chem.*, vol. 78, no. 26, pp. 2673–2677, Dec. 1974.
[7] M. I. Ojovan, "Viscosity and glass transition in amorphous oxides," *Adv. Condens. Matter Phys.*, vol. 2008, 2008, Art. ID. 817829.
[8] Y. Wang, X. Bian, and R. Jia, "Effects of cooling rate on thermal expansion of $Cu_{49}Hf_{42}Al_9$ metallic glass," *Trans. Nonferrous Metals Soc. China*, vol. 21, no. 9, pp. 2031–2036, 2011.
[9] D. Turnbull and M. H. Cohen, "Free-volume model of the amorphous phase: Glass transition," *J. Chem. Phys.*, vol. 34, no. 1, pp. 120–125, Jan. 1961.
[10] M. H. Lai *et al.,* "Thermal stress modification in regenerated fiber Bragg grating via manipulation of glass transition temperature based on CO_2-laser annealing," *Opt. Lett.*, vol. 40, no. 5, pp. 748–751, Mar. 2015.
[11] G. Meltzand and W. W. Morey, "Bragg grating formation and germanosilicate fiber photosensitivity," in *Proc. SPIE Int. Workshop Photoinduced Self-Org. Effects Opt. Fiber*, 1991, vol. 1516, p. 185.

[12] P. C. Hill, G. R. Atkins, J. Canning, G. C. Cox, and M. G. Sceats, "Writing and visualization of low-threshold type II Bragg gratings in stressed optical fibers," *Appl. Opt.*, vol. 34, no. 33, pp. 7689–7694, Nov. 1995.
[13] I. Abe *et al.,* "Production and characterization of refractive index gratings in high-birefringence fiber optics," *Opt. Lasers Eng.*, vol. 39, no. 5/6, pp. 537–548, May/Jun. 2003.
[14] I. Abe, H. J. Kalinowski, R. Nogueira, J. L. Pinto, and O. Frazao, "Production and characterisation of Bragg gratings written in high-birefringence fiber optics," *Proc. Inst. Elect. Eng.—Circuits, Devices Syst.*, vol. 150, no. 6, pp. 495–500, Dec. 2003.
[15] A. Siekieraa, R. Engelbrecht, R. Neumann, and B. Schmauss, "Fiber Bragg gratings in polarization maintaining specialty fiber for Raman fiber lasers," *Phys. Procedia*, vol. 5, pp. 671–677, 2010.
[16] E. Chehura, C. C. Ye, S. E. Staines, S. W. James, and R. P. Tatam, "Characterization of the response of fiber Bragg gratings fabricated in stress and geometrically induced high birefringence fibers to temperature and transverse load," *Smart Mater. Struct.*, vol. 13, no. 9, pp. 888–895, Jun. 2004.
[17] L. A. Ferreira, F. M. Araujo, J. L. Santos, and F. Farahi, "Simultaneous measurement of strain and temperature using interferometrically interrogated fiber Bragg grating sensors," *Opt. Eng.*, vol. 39, no. 8, pp. 2226–2234, Aug. 2000.
[18] G. H. Chen *et al.,* "Simultaneous strain and temperature measurements with fiber Bragg grating written in novel Hi-Bi optical fiber," *IEEE Photon. Technol. Lett.*, vol. 16, no. 1, pp. 221–223, Jan. 2004.
[19] C. C. Ye, S. E. Staines, S. W. James, and R. P. Tatam, "A polarization-maintaining fiber Bragg grating interrogation system for multi-axis strain sensing," *Meas. Sci. Technol.*, vol. 13, no. 9, pp. 1446–1449, Aug. 2002.
[20] T. Mawatari and D. Nelson, "A multi-parameter Bragg grating fiber optic sensor and triaxial strain measurement," *Smart Mater. Struct.*, vol. 17, no. 3, May 2008, Art. ID. 035033.
[21] C. M. Lawrence, D. V. Nelson, E. Udd, and T. Bennett, "A fiber optic sensor for transverse strain measurement," *Exp. Mech.*, vol. 39, no. 3, pp. 202–209, Sep. 1999.
[22] C. L. Zhao *et al.,* "Switchable multi-wavelength erbium-doped fiber lasers by using cascaded fiber Bragg gratings written in high birefringence fiber," *Opt. Commun.*, vol. 230, no. 4–6, pp. 313–317, Feb. 2004.
[23] Y. G. Liu, X. H. Feng, S. Z. Yuan, G. Y. Kai, and X. Y. Dong, "Simultaneous four-wavelength lasing oscillations in an erbium-doped fiber laser with two high birefringence fiber Bragg gratings," *Opt. Exp.*, vol. 12, no. 10, pp. 2056–2061, May 2004.
[24] C. Spiegelberg *et al.,* "Low-noise narrow-linewidth fiber laser at 1550 nm (June 2003)," *J. Lightw. Technol.*, vol. 22, no. 1, pp. 57–62, Jan. 2004.
[25] F. Yang *et al.,* "Orthogonal polarization mode coupling for pure twisted polarization maintaining fiber Bragg gratings," *Opt. Exp.*, vol. 20, no. 27, pp. 28839–28845, Dec. 2012.
[26] G. A. Pavlath and H. J. Shaw, "Birefringence and polarization effects in fiber gyroscopes," *Appl. Opt.*, vol. 21, no. 10, pp. 1752–1757, May 1982.
[27] K. S. Lim, C. H. Pua, S. W. Harun, and H. Ahmad, "Temperature-sensitive dual-segment polarization maintaining fiber Sagnac loop mirror," *Opt. Laser Technol.*, vol. 42, no. 2, pp. 377–381, Mar. 2010.
[28] A. J. Barlow, "Optical-fiber birefringence measurement using a photo-elastic modulator," *J. Lightw. Technol.*, vol. 3, no. 1, pp. 135–145, Feb. 1985.
[29] M. H. Lai, D. S. Gunawardena, K. S. Lim, H. Z. Yang, and H. Ahmad, "Observation of grating regeneration by direct CO2 laser annealing," *Opt. Exp.*, vol. 23, no. 1, pp. 452–463, Jan. 2015.